Light Harvesting by Carotenoids Incorporated into the B850 Light-Harvesting Complex from *Rhodobacter sphaeroides* R-26.1: Excited-State Relaxation, Ultrafast Triplet Formation, and Energy Transfer to Bacteriochlorophyll

Emmanouil Papagiannakis,*,† Somes Kumar Das,‡ Andrew Gall,§ Ivo H. M. van Stokkum,† Bruno Robert,|| Rienk van Grondelle,† Harry A. Frank,‡ and John T. M. Kennis*,†

Department of Biophysics, Division of Physics and Astronomy, Vrije Universiteit, De Boelelaan 1081, 1081 HV, Amsterdam, The Netherlands, Department of Chemistry, 55 North Eagleville Road, University of Connecticut, Storrs, Connecticut 06269-3060, Division of Biochemistry and Molecular Biology, IBLS, University of Glasgow, Glasgow G128QQ, United Kingdom, and Service de Biophysique des fonctions Membranaires, DBJC/CEA et URA CNRS 2096, CEA Saclay, 91191 Gif/Yvette Cedex, France

Received: October 9, 2002; In Final Form: April 4, 2003

Spirilloxanthin and spheroidene were reconstituted into the carotenoidless B850 light-harvesting (LH) complex from the *Rhodobacter* (*Rb*.) *sphaeroides* R-26.1 mutant with the aim to obtain new insights in energy transfer, triplet formation, and other relaxation phenomena in photosynthetic light harvesting. Resonance Raman measurements showed that spirilloxanthin and spheroidene are bound to the B850 complex in the same planar configuration, whereas spirilloxanthin in its native LH1 complex of *Rhodospirillum* (*Rs*.) *rubrum* assumes a twisted configuration. Ultrafast transient absorption measurements with excitation of the carotenoid molecules to their S_2 state enabled us to identify, in both reconstituted B850 complexes, the recently found S* carotenoid singlet excited state and the direct generation of carotenoid triplet states within picoseconds through the singlet fission mechanism [Gradinaru, C. C., et al. *Proc. Natl. Acad. Sci. U.S.A.* **2001**, *98*, 2364−2369]. Global analysis has allowed us to quantify the formation yields of these states. In the B850 complex reconstituted with spheroidene, the triplet yield is 5−10%, similar to that found on the spheroidene-binding LH2 complex of *Rb. sphaeroides* 2.4.1 [Papagiannakis, E. et al. *Proc. Natl. Acad. Sci. U.S.A.* **2002**, *99*, 6017−6022]. The triplet state of spirilloxanthin in the B850 complex is formed with a similar low yield, in contrast to the native LH1 complex of *Rs. rubrum* where the triplet yield is as large as 25−30%. This illustrates that the formation of the triplet state depends on the type of complex that binds the carotenoid and not on the carotenoid itself. More specifically, the singlet fission process that underlies ultrafast triplet formation is more efficient when spirilloxanthin is bound in a distorted configuration (in *Rs. rubrum*) than with either spirilloxanthin or spheroidene bound in a planar configuration (in *Rb. sphaeroides*). The extent of geometrical deformation of the carotenoid imposed by binding to the LH complexes partly determines the carotenoid light-harvesting function by either deactivating the excited-state energy of S* by transformation into a triplet pair or allowing this energy to flow to bacteriochlorophyll. Comparison of the energy transfer properties in the spheroidene-reconstituted B850 complex, which lacks the B800 bacteriochlorophyll, with that of the LH2 complex of *Rb. sphaeroides* 2.4.1 suggests that, apart from a light-harvesting function, the B800 bacteriochlorophylls in LH2 may have an important role in funneling the photon energy absorbed by carotenoids toward the reaction center.

Introduction

Purple photosynthetic bacteria utilize a highly organized photosynthetic apparatus, comprising two kinds of antenna light harvesting (LH) complexes, LH1 and LH2.[1] The LH1 complex is closely associated with the reaction center where light-induced electron transfer takes place, whereas the LH2 is located peripherally. The LH complexes are structurally highly organized and have a specific carotenoid: bacteriochlorophyll (BChl) pigment stoichiometry of 1:2 in LH1[2] and 1:3 in LH2.[3] The crystal structure of the LH2 complex shows an overall cylindrical shape and reveals the existence of two distinct rings of BChls, which give rise to characteristic absorption peaks at 800 and 850 nm.[3] The structure of the minimal unit is an $\alpha\beta$ heterodimer that binds three BChls, two of which are part of the B850 ring while the third is part of the B800 ring. Each unit binds one carotenoid, which is in close proximity with all BChls. Carotenoids play an important role for photosynthetic bacteria because they harvest sunlight from the blue-green spectral region where BChl shows minimal absorption. Carotenoids make the energy that they absorb available to the organism by transferring it to neighboring BChls from where it ultimately makes its way to the reaction center.[4−6]

Absorption of a photon in the 450−550 nm region promotes carotenoids from their ground electronic state S_0 (with an $1A_g^-$ symmetry) to the singlet $1B_u^+$ state, traditionally referred to as the S_2 state. The transition from S_0 to the lower $2A_g^-$ singlet

* To whom correspondence should be addressed. E-mail: papagian@nat.vu.nl or john@nat.vu.nl. Fax: +31-20-4447999.
† Vrije Universiteit.
‡ University of Connecticut.
§ University of Glasgow.
|| Service de Biophysique des fonctions Membranaires.

10.1021/jp027174i CCC: $25.00
Published on Web 05/17/2003

state (S_1) is one-photon-forbidden according to symmetry selection rules. Recently, we have shown that there exists another singlet state of low energy, of unknown symmetry properties, which we have termed S*.[7] The S_1 and S* states are populated in parallel after internal conversion (IC) from S_2, which typically takes place within 150 fs.[7,8] S_1 decays to the ground state by IC, with a lifetime that depends on the conjugation length of the carotenoid,[9] whereas S* is a precursor in the formation of carotenoid triplets generated on a picosecond time scale. The S* state may correspond to one of the covalent $1B_u^-$ or $3A_g^-$ polyene states predicted to be lower in energy than S_2 for long carotenoids.[11] Following the theoretical work by Tavan and Schulten,[11] we proposed that the ultrafast triplet formation proceeded via the intramolecular singlet fission mechanism, whereby a singlet excitation separates into a pair of triplet states, localized on separate segments of the polyene chain and with their spins correlated to maintain a singlet spin state. The probability of this localization process would depend strongly on the degree of conformational distortion of the polyene backbone.[7,11]

Investigations of the light-harvesting function of carotenoids in bacterial antenna complexes have shown that energy can be transferred to BChl from both S_1[12,13] and S_2,[14] depending on the protein complex and its carotenoid composition. Systematic study of carotenoids with increasing conjugation length and of LH complexes with variation only in their carotenoid content has provided information about the role that the conjugation length plays in excitation energy transfer (EET) by influencing both the energy and the lifetime of the S_1 state.[9,15] Efficient energy transfer demands that the channel from S_1 be active, which is typically the case for carotenoids with up to 10 conjugated double bonds, such as spheroidene in the LH2 complex of *Rhodobacter* (*Rb.*) *sphaeroides* 2.4.1. Recently, we demonstrated that the EET efficiency of more than 90% in that complex is achieved by the employment of an additional energy transfer pathway involving S*.[8] Thus, the S* state is capable of transferring singlet excited-state energy to BChl and does so in competition with the singlet fission process that leads to ultrafast triplet generation. The conclusion that the carotenoid triplet generation and the EET transfer process to BChl are two competing processes having S* as a common parent state is supported by earlier magnetic field effect studies, which have shown that the presence of a magnetic field causes a decrease of the carotenoid triplet yield and a concomitant increase of the BChl fluorescence in *Rb. sphaeroides* 2.4.1.[16]

The conformation of the carotenoids is dictated by the protein scaffolding of the LH complexes, and as previous resonance Raman (RR) studies have demonstrated, even though carotenoids assume an *all-trans* conformation in the LH complexes, various degrees of carotenoid backbone twisting may occur in complexes of different species.[15,17] Notably, a study encompassing a number of purple bacterial species indicated that LH complexes binding carotenoids in a planar configuration exhibited a significantly higher light harvesting efficiency through their carotenoids than LH complexes binding twisted carotenoids.[17]

Spirilloxanthin is the primary carotenoid bound to the LH1 complex of *Rhodospirillum* (*Rs.*) *rubrum* where it assumes a significantly twisted form, whereas spheroidene is bound in a less twisted, planar form in the LH2 complex of *Rb. sphaeroides* 2.4.1.[17] These studies have shown that the configuration of carotenoids reconstituted into carotenoidless LH complexes did not depend on the conjugation length of the carotenoids. We have proposed that the conformational distortion of spirilloxanthin in the LH1 complex of *Rs. rubrum* results in a remarkably high (25−30%) spirilloxanthin triplet yield via singlet fission from S*.[7] In the LH2 complex of *Rb. sphaeroides* 2.4.1, which binds spheroidene in a planar way, the triplet state of spheroidene is also formed via the same mechanism, but with a lower yield, 5%.[8]

To make a systematic study and comparison of the configuration and the spectroscopic properties of spirilloxanthin and spheroidene in the different types of LH complexes, we incorporated these carotenoids into the carotenoidless LH2-type B850 complex of *Rb. sphaeroides* R-26.1. We employed resonance Raman spectroscopy to determine the configuration of the carotenoids when bound to the LH complexes. Ultrafast transient absorption measurements and subsequent global analysis enabled us to quantify the dynamic processes in the different complexes, and disentangle energy transfer, internal conversion, and singlet fission processes, allowing for an assessment of the relation between triplet formation by singlet fission and the protein-imposed carotenoid configuration. The differences in the spheroidene-BChl EET pathways between the B850 complex of *Rb. sphaeroides* R-26.1 reconstituted with spheroidene and the LH2 complex of *Rb. sphaeroides* 2.4.1 that was studied previously[8] shed light on the role that the B800 BChls play in the EET process from carotenoids to BChl in LH2.

Materials and Methods

Sample Preparation. The preparation of the *Rb. sphaeroides* R-26.1 B850 complexes and subsequent incorporation of the carotenoids was conducted according to previously published procedures,[15] with the following modification: After sonification with 15 molar excess carotenoids, the reaction mixture was stirred for 2 h on ice in the dark. Then, the deoxycholate concentration was reduced from 2% to 0.02% by overnight dialysis at 4 °C using a 15 mM Tris buffer at pH 8.0 containing 0.02% deoxycholate.

Experimental. Resonance Raman spectra were recorded on a Jobin-Yvon U1000 double-monochromator Raman spectrometer, equipped with N_2-cooled, back-thinned, ultra-sensitive charge-coupled-device detector (Spectrum One, Jobin-France), on samples maintained at 77 K in an SMC-TBT nitrogen-flow cryostat (Air−Liquide, France). Excitation at 514.5 nm was provided by a Coherent Innova 100 Argon laser.

Ultrafast transient absorption spectroscopy was performed as described earlier in detail.[18] In brief, an amplified Ti:sapphire laser system (Coherent-BMi α1000) operating at 1 kHz with pulse width of 70 fs at 800 nm was used to pump a noncollinear optical parametric amplifier (NOPA) which provided tunable pulses for selective excitation of the S_2 state of the carotenoids. A fraction of the 800 nm light was driven through an optical delay line and subsequently focused on a 2-mm sapphire plate to create a single-filament white light continuum, which was split into probe and reference beams. The pump and probe beams were focused to a spot of 200-μm diameter in the sample. A double-diode-array detector was used to read probe and reference spectra after dispersion of the beams by a polychromator, typically covering the entire visible spectrum. The *Rb. sphaeroides* R-26.1 B850 complex reconstituted with spheroidene (B850:sph) was kept in a 1-mm quartz cuvette and the B850 complex reconstituted with spirilloxanthin (B850:spx) in a 2-mm quartz cuvette, which were continuously shaken to avoid degradation of the sample by exposure to multiple laser shots. The excitation energy was 50 nJ per pulse for the B850:sph complex, whereas for B850:spx, due to the low amount of spirilloxanthin, it was necessary to use a higher energy, 300 nJ

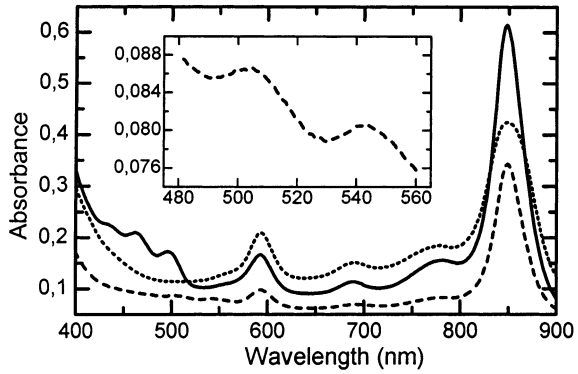

Figure 1. Absorption spectra of the carotenoid-less B850 complex of *Rb. sphaeroides* R-26.1 (dotted line), the same complex reconstituted with spheroidene (solid line) and spirilloxanthin (dashed line). The inset shows the absorption peaks of spirilloxanthin in magnification.

per pulse. The transient absorption spectrum of the carotenoid-less B850 complex of *Rb. sphaeroides* R-26.1 was measured after excitation at 500 nm by pulses of 300 nJ.

Data Analysis. The measured data were globally analyzed.[7,8,19] The fitting procedure takes into account the group velocity dispersion of the probe white light and the convolution with the instrument response function, which is typically 120 fs (fwhm). In short, the transient absorption spectra that were obtained for a specific sample (typically 150) were fitted simultaneously, and the decay lifetimes were estimated. A model was applied, following the assumption that the data can be described using a sequential scheme of species that evolve with a specific lifetime into another, i.e., A → B → C → D → ..., each species possessing a species-associated difference spectrum (SADS). The lifetimes and SADS are used to provide a description of the spectral and temporal evolution present in the data and do not need to be necessarily associated with pure (excited) states.

Results

The successful incorporation of spheroidene in the *Rb. sphaeroides* R-26.1 B850 complex has been demonstrated earlier.[20] The resulting complex, hereafter referred to as B850:sph, resembles the LH2 complex of *Rb. sphaeroides* 2.4.1 but lacks the 800-nm absorbing BChls, as seen in the absorption spectrum (Figure 1, solid line). The absorption of the *Rb. sphaeroides* R-26.1 B850 complex reconstituted with spirilloxanthin, referred to as B850:spx, is shown in Figure 1 by the dashed line. The incorporation level of spirilloxanthin in the B850:spx complex is rather low, on the order of 5−10%. The distinct peaks in the absorption spectrum at 505 and 542 nm, significantly red-shifted with respect to that in solution,[7] indicate that spirilloxanthin has been successfully incorporated in a well-defined environment (Figure 1, inset). The dotted line of Figure 1 indicates the absorption of the native, carotenoidless *Rb. sphaeroides* R-26.1 B850 complex.

Resonance Raman Spectra of the LH Complexes in the ν_4 Region. We applied RR spectroscopy to study and compare the configuration of spirilloxanthin in the *Rs. rubrum* LH1 complex to that of spirilloxanthin and spheroidene in the reconstituted *Rb. sphaeroides* R-26.1 B850 complexes. The samples were cooled to 77 K, and the RR spectra of all complexes were induced by excitation light of 514.5 nm. The carotenoid RR spectrum around 960 cm^{-1} (ν_4 region) is characteristic for the out-of-plane wag of C−H, which only becomes symmetry-allowed upon nonplanar distortions of the polyene backbone. On the other hand, the ν_3 region around 1000 cm^{-1}, representing $C-CH_3$ vibrations, is insensitive to such deformations, and the amplitude of the ν_4 feature relative to the ν_3 peak can be utilized as a measure of the twist of the carotenoids in the LH complexes.[17,21,22]

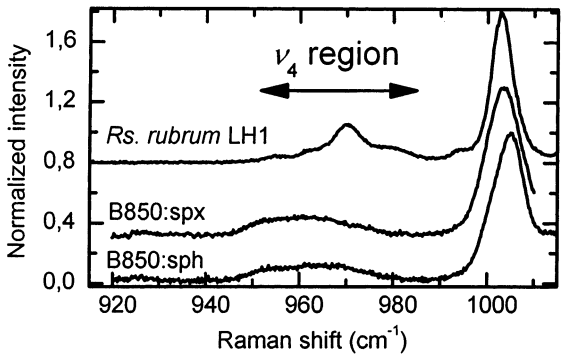

Figure 2. Comparison of the ν_4 region resonance Raman spectra induced by excitation at 514.5 nm of the *Rb. sphaeroides* R-26.1 B850:sph, B850:spx and the *Rs. rubrum* LH1 complexes.

The ν_4 region of the RR spectrum of the *Rs. rubrum* LH1 complex is quite intense and has distinct structure, comprising several narrow features that appear at 954, 961, 968, and 978 cm^{-1} (Figure 2). The discrete ν_4 peaks originate from twists at specific regions of the polyene backbone, probably at the $C_{11}=C_{12}$ and $C_7=C_8$ positions (and their symmetric $C_{11'}=C_{12'}$ and $C_{7'}=C_{8'}$),[23] suggesting that spirilloxanthin assumes a specific, twisted configuration when bound to the LH1 complex of *Rs. rubrum*. On the other hand, as seen in Figure 2, the ν_4-region RR spectra of both of the B850:sph and the B850:spx complexes contain only a weak, broad, and featureless band over the 950−970 cm^{-1} region. Desamero et al. have previously shown that the RR spectrum of spheroidene in the B850:sph complex is essentially the same as that of the LH2 complex of *Rb. sphaeroides* 2.4.1.[15] Evidently, both spirilloxanthin and spheroidene are maintained by the *Rb. sphaeroides* LH proteins in a similar, planar configuration, contrary to spirilloxanthin in the LH1 protein of *Rs. rubrum* where it is significantly twisted.

Ultrafast Transient Absorption Measurements. *Spheroidene Dynamics in the B850 Complex.* The S_2 state of spheroidene was selectively excited by 500-nm laser pulses, whereas the spectral changes that followed excitation were probed throughout the visible region. Figure 3 shows time-resolved spectra at selected time delays. The excited-state absorption (ESA) of S_1 appears soon after excitation and peaks at 550 nm with a pronounced shoulder at 525 nm. Within a few picoseconds, the 550-nm peak decays while the 525-nm feature remains intact and a BChl bleach, indicative of EET, is present at 595 nm. The 2-ns spectrum contains only an absorption feature near 525 nm. The bleach at 595 nm has disappeared, which indicates that the excited states on BChl have decayed. The measured data requires no less than five components for a satisfactory description. Figure 4 shows selected traces measured at 525, 551, and 571 nm and the respective fits from global analysis. Following our previous study on the LH2 complex of *Rb. sphaeroides* 2.4.1,[8] we can relate the decay components to the specific processes that take place in the antenna. Application of a sequential model in the global analysis provides an estimate of the SADS of each component. In this way, we can visualize and relate the spectral changes that were evident in the transient absorption spectra to evolutionary lifetimes.

The instantaneously appearing SADS, which decays with a sub-100-fs lifetime, has negative features throughout the visible region (Figure 5). A peak around 510 nm corresponds to the

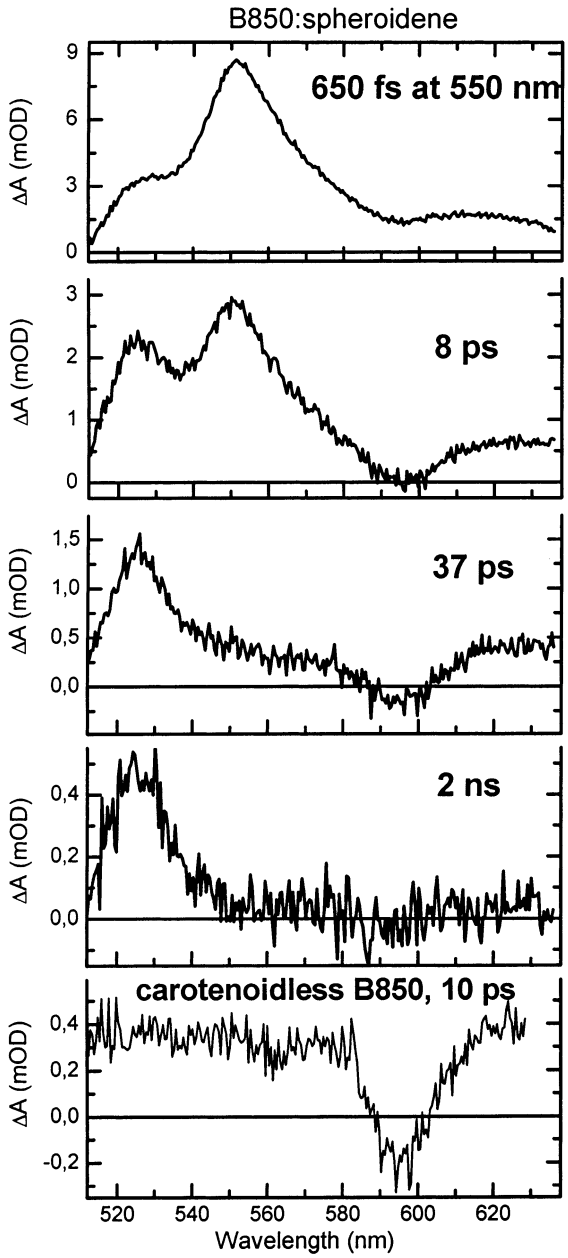

Figure 3. Transient absorption spectra measured on the B850 complex of *Rb. sphaeroides* R26.1 reconstituted with spheroidene, after excitation of spheroidene to the S_2 state. The first spectrum corresponds to the pump−probe delay of the maximum signal of the S_1-S_n excited-state absorption and the others to delays of 8 ps, 37 ps, and 2 ns. These are the raw time-resolved spectra, uncorrected for the group-velocity dispersion of the probe light. In the top spectrum, the 550-nm peak corresponds to a pump−probe delay of 650 fs. For the later spectra, the effect of the group velocity dispersion (700 fs over the entire spectral range) is negligible. The lowest panel shows, for comparison, the ΔA spectrum measured after excitation in the carotenoid region of the carotenoidless B850 complex of *Rb. sphaeroides* R-26.1 at a delay of 10 ps. Note the different vertical scale of each graph.

ground-state bleaching of spheroidene, and the broad negative band extending to 635 nm is due to stimulated emission (SE) originating from the S_2 state. The 2nd SADS contains a very broad ESA peaking at 560 nm, which covers the ESA region of the S* and S_1 states and decays in 500 fs. According to our previous model,[8] this SADS describes the ESA of the S* state and the vibrationally hot S_1 state, which are formed simultaneously after the depopulation of S_2. The evolution from the 2nd to the 3rd SADS in 500 fs involves a substantial loss of

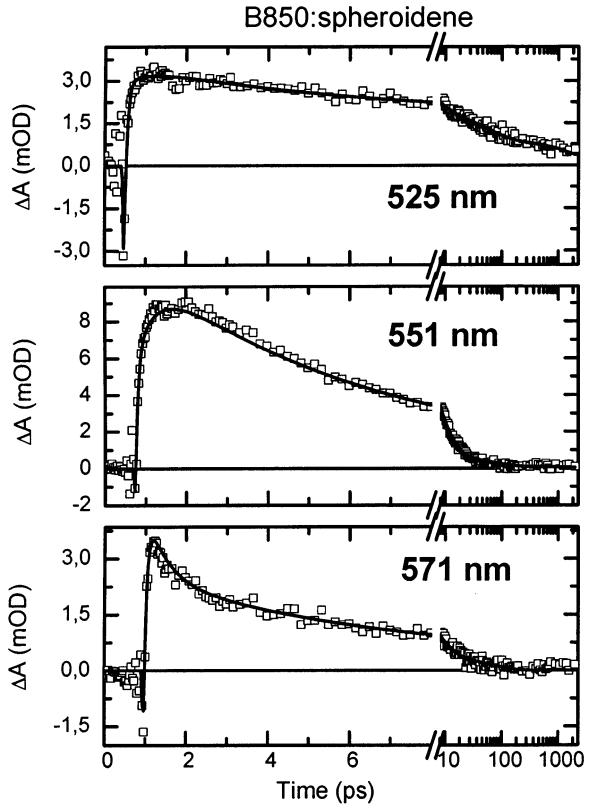

Figure 4. Some characteristic kinetic traces measured on the *Rb. sphaeroides* R-26.1 B850 complex reconstituted with spheroidene. The top trace corresponds to the peak of the S* ESA (525 nm), the middle trace corresponds to the peak of the S_1 ESA (551 nm), and the lowest trace corresponds to the red wing of the S_1 ESA (571 nm). The solid lines indicate the fit of the data to five lifetimes and corresponds to the SADS shown in Figure 4.

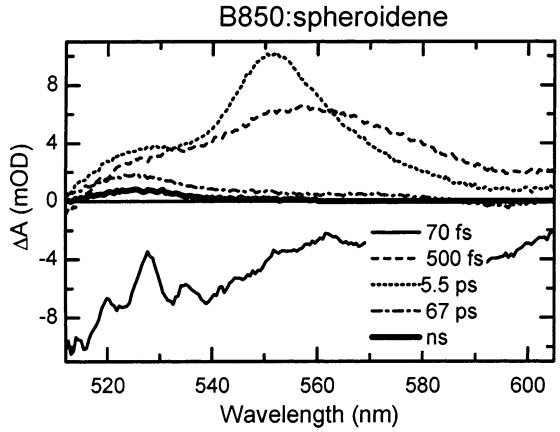

Figure 5. SADS and associated lifetimes of the *Rb. sphaeroides* R-26.1 B850 complex reconstituted with spheroidene.

ESA in the region above 565 nm and a large gain of ESA in the 540−560 nm region (see also the kinetic traces in Figure 4). The 3rd SADS, which represents a decay of the S_1/S* ESA, has a 5.5 ps lifetime, which is shorter than the lifetime of S_1 of spheroidene in hexane (8.5 ps)[9] and longer than that in the LH2 complex of *Rb. sphaeroides* 2.4.1 (1.5 ps).[8,12] This indicates that in the B850:sph complex energy transfer from S_1 to BChl does take place, but at a slower rate than in the LH2 complex of 2.4.1[8]. The 4th SADS includes an ESA feature at 525 nm and a broad ESA extending toward the red and has a lifetime of 67 ps. A small bleach around 595 nm indicates the presence of excited BChl molecules. The decay of this SADS describes

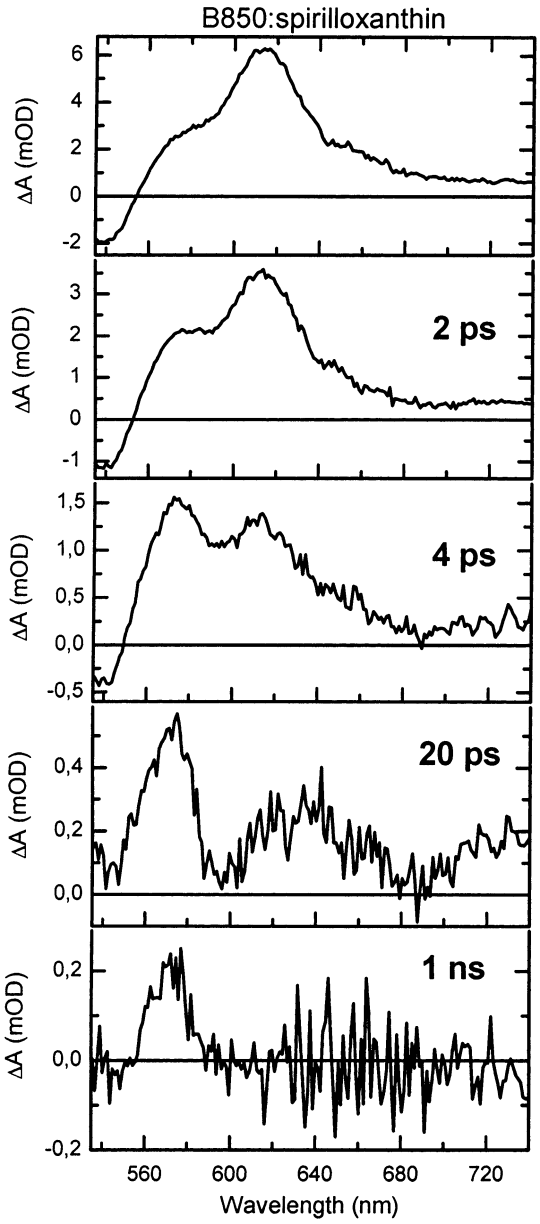

Figure 6. Transient absorption spectra measured on the B850 complex of *Rb. sphaeroides* R-26.1 reconstituted with spirilloxanthin. The first spectrum corresponds to the pump−probe delay of maximum signal for the S_1-S_n excited-state absorption and the others to delays of 2 ps, 4 ps, 20 ps, and 1 ns. Note that these are the raw time-resolved spectra, uncorrected for group velocity dispersion (see Figure 2).

a significant loss of amplitude of the 525 nm ESA and the disappearance of the 595 nm bleach. The lifetime of 67 ps, which is similar to one found in the LH2 complex of *Rb. sphaeroides* 2.4.1,[8] probably corresponds to a relaxation of the spheroidene triplet mixed with the decay dynamics of BChl. The final, 5th SADS is a long-lived species containing only the absorption peak at 525 nm which we ascribe to the triplet state of spheroidene,[15] which is the only excited species still present after 2 ns. Notably, the relative amplitude of this SADS is very similar to that of the respective SADS in the LH2 complex of *Rb. sphaeroides* 2.4.1,[8] indicating that the triplet yield is comparable in the two complexes.

Spirilloxanthin Dynamics in the B850 Complex. Spirilloxanthin is the only carotenoid studied so far for which the presence of the S* state was demonstrated in solution. Moreover, when bound to the LH1 complex of *Rs. rubrum*, spirilloxanthin shows

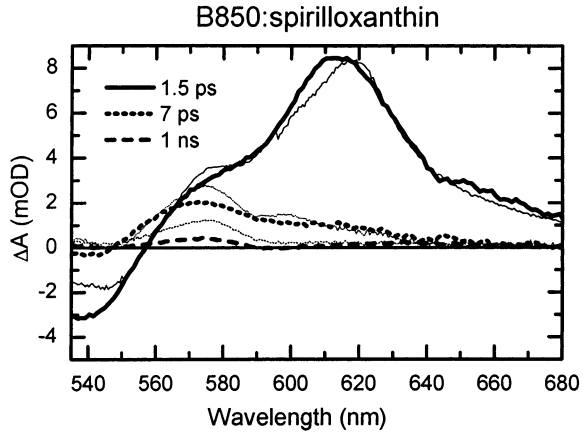

Figure 7. Sequential SADS and associated lifetimes of the B850 complex of *Rb. sphaeroides* R-26.1 reconstituted with spirilloxanthin. The respective SADS of the *Rs. rubrum* LH1 complex which also contains spirilloxanthin are shown in thin lines for comparison, normalized at the maximum of the S_1 absorption (taken from ref 7).

a particularly high (25−30%) triplet yield after direct excitation.[7] Incorporating it into the B850 complex of *Rb. sphaeroides* R-26.1, where it experiences a different environment compared to the native LH1 complex of *Rs. rubrum*, allows us to investigate the role of the protein matrix in the formation of the S* and the triplet states and its influence on the S_1 state. Spirilloxanthin was excited into the S_2 state by 520-nm laser pulses.

The transient absorption spectra recorded on the B850:spx complex (Figure 6) reveal a spectral evolution bearing similarities to those observed in the LH1 and LH2 complexes studied previously.[7,8] The ESA of spirilloxanthin dominates in the visible region shortly after excitation and contains two main characteristic features, at 615 and 575 nm, with the former disappearing in about a picosecond and the latter decaying significantly slower. At intermediate delays, a small BChl bleach feature is present at 595 nm, implying that some energy transfer from spirilloxanthin to BChl has taken place. The long-lived spectra contain only a small positive feature at 575 nm, which we ascribe to the absorption of the spirilloxanthin triplet.[7,10] Comparison of this spectrum with the spectrum measured on the carotenoidless R-26.1 B850 complex (Figure 3) confirms that the 575-nm feature is not due to excited BChl.

A four-component model is necessary to fit the data adequately, yielding lifetimes of sub-100 fs, 1.5 ps, 7 ps, and a long-lived component. Figure 7 shows the resulting SADS. The sub-100 fs component appeared unreliable owing to a cross-phase modulation signal around time-zero resulting from the relatively high excitation power and is not shown. The SADS of the intermediate species with a lifetime of 1.5 ps has a shape identical to the analogous SADS estimated for the LH1 complex of *Rs. rubrum* (also shown for comparison). It shows a maximum at 620 nm and a shoulder at 575 nm, which correspond to the ESA of the S_1 and S* states which coexist after the relaxation of S_2. The next state corresponds to a SADS that shows only the band around 575 nm, which, like in LH1 of *Rs. rubrum*,[7] can be assigned to the presence of the S* state. The 7-ps lifetime is similar to that in the LH1 complex, indicating the common nature of this process in the two complexes. The final SADS, which is associated with the absorption of the triplet state of spirilloxanthin, remains present for times beyond the range of our apparatus (2 ns). The amplitude of this SADS compared to the related one in the

Rs. rubrum LH1 complex indicates that the triplet in the B850:spx complex is formed with a significantly smaller, 3-fold lower yield.

Discussion

Energy Flow in the B850:sph Complex. Excitation of spheroidene to its S_2 state in B850:sph is followed by the parallel decay via IC to the S_1 and S* states, and EET to BChl. It was shown that in the LH2 complex of *Rb. sphaeroides* 2.4.1, an unrelaxed, or "hot", S_1 state is formed after the depopulation of S_2. A similar process is evident in the B850:sph complex (Figure 5, spectral evolution from 2nd to 3rd SADS); however, it shows marked spectral differences with respect to that observed in the LH2 complex of *Rb. sphaeroides* 2.4.1.[8] In the latter case, the S_1 peak at 555 nm was already present in the initial spectrum and a fast, 300 fs, decay component represented a loss of longer-wavelength ESA in a non-conservative fashion, indicating that energy transfer occurs from the hot S_1 state. Unlike the results for *Rb. sphaeroides* 2.4.1, the relaxation process in the B850:sph complex is conservative, implying that in this case no energy transfer occurs from the hot S_1 state. It may tentatively be concluded that, in the LH2 complex of *Rb. sphaeroides* 2.4.1., the B800 BChl is the main acceptor of energy from the hot S_1 state. The Q_y level of the B800 BChls, which energetically lies higher than the Q_y level of the B850 BChls, may have a better spectral overlap with the hot S_1 state of spheroidene and, possibly, a more favorable orientation. The longer lifetime of the cooling process is another indication of the lack of energy transfer. In the LH2 complex of *Rb. sphaeroides* 2.4.1, it is 300 fs,[8] whereas in the B850:sph complex, it is 500 fs.

The ESA feature that appears at 525 nm soon after excitation indicates that, like in the LH2 complex of *Rb. sphaeroides* 2.4.1, the S* state of spheroidene is populated in the B850:sph complex as well. However, it is not possible to distinguish the S* from the S_1 dynamics because their lifetimes are similar, and therefore, we cannot decipher the exact energy transfer pathways as for the LH2 complex of *Rb. sphaeroides* 2.4.1.[8] The shortening of the S_1 lifetime from 8.5 ps in solution to 5.5 ps in the B850:sph complex indicates that EET transfer occurs from the relaxed S_1 to BChl, at 35% efficiency. This is significantly less efficient than in the LH2 complex of *Rb. sphaeroides* 2.4.1 where the S_1 state transfers energy to BChl by 85%,[8,12] indicating that the B800 BChl plays a significant role in this pathway of EET. Desamero et al.[15] have reported a longer lifetime for the S_1 state of spheroidene in the B850:sph complex, 7.9 ps, essentially the same lifetime as for spheroidene in solution, implying that no or very little EET from S_1 to BChl occurs. The origin of the difference from our results is unclear, but we note that in the study of Desamero et al. the S_1 lifetime was estimated from a single wavelength trace which, compared to an analysis of the full spectrum of the measurements presented here, carries significantly less information. Our results are in line with those reported by MacPherson et al., who observed a decrease of the light-harvesting efficiency of rhodopin glucoside in a B800-deficient LH2 complex of *Rps. acidophila*.[14] In this LH2 complex, the EET process to BChl proceeds almost exclusively through the S_2 state. Our results indicate that B800 is a major acceptor not only from the S_2 state, but from S_1 and possibly from S* as well, suggesting that apart from a direct light-harvesting function, the B800 BChls in LH2 may have an important function by enabling an efficient transfer of photon energy absorbed by carotenoids to low-energy BChls.

Given the 52% EET efficiency of spheroidene in the B850:sph complex,[15] the paths that include B800 are likely to account for the remaining 40% of the total energy transfer in the LH2 complex of *Rb. sphaeroides* 2.4.1. Therefore, if we take into account the efficiencies that were estimated for the different pathways of EET in that complex,[8] and exclude the pathways involving the B800, we can conclude that in the B850:sph complex the S_2 state of spheroidene is ~25% efficient in direct EET to BChl (compared to 57% in the LH2 of 2.4.1). Assuming that the S_1/S* formation yield is preserved, then the S_1 state is formed with ~45% and the S* with ~30% yield. The shortening of the S_1 lifetime shows that it is transferring ~35% of its energy to B850, thus accounting for 15% of the total energy reaching BChl. According to our previous estimations,[8] in absence of the B800 BChls, the S* state must be transferring very little energy to BChl, of the order of 5% or less. These estimations bring the total EET efficiency in the B850:sph complex to ~45%, close to the 52% reported by Desamero et al.[15]

Energy Flow in the B850:spx Complex. The excitation of spirilloxanthin in the B850:spx complex initiates a spectral evolution very similar to that in the LH1 complex of *Rs. rubrum*.[7] The energy transfer to BChl is inefficient, as implied by the small magnitude of the BChl bleach signal at 595 nm observed 20 ps after excitation of spirilloxanthin (Figure 6), which is actually comparable to that measured under similar excitation conditions in the carotenoidless B850 complex (Figure 3).

The excitation to the S_2 state is followed by the population, in parallel, of the lower singlet excited states S_1 and S*, which then decay with lifetimes of 1.5 and 7 ps, respectively, similarly to the LH1 complex of *Rs. rubrum*.[7] Unlike spheroidene in the B850:sph complex, a sub-ps S_1 relaxation component, attributable to a vibrational cooling process, is not observed for spirilloxanthin. In spirilloxanthin measurements in solution, this component has been observed, but it has a lifetime as short as 200 fs;[24] therefore, it is very likely that in the current measurements it is obscured by the cross phase modulation signal around time-zero.

The 7 ps lifetime of S* in B850:spx is very close to the 5 ps found in the LH1 complex,[7] suggesting that its dynamic properties in the two complexes do not differ significantly. The S_1 and the S* states are temporally well separated, making the estimation of their SADS sound and therefore the determination of the formation yields of S* and the triplet by a direct comparison of their amplitudes in the two different complexes is plausible. By comparing the magnitudes of the respective SADS in the B850:spx and *Rs. rubrum* LH1 complexes (Figure 7), we find that in the B850:spx complex the S* signal is decreased by approximately 25% and the triplet signal by 65%. Therefore, we can conclude that a significant difference between the properties of B850:spx and LH1 is the 3-fold decrease of the triplet yield. In the B850:spx complex, the triplet yield of spirilloxanthin is of the order of 5−10%, which brings it closer to the triplet yield of spheroidene in B850:sph than to that of spirilloxanthin itself in the LH1 complex of *Rs. rubrum*.

Effect of Carotenoid Configuration on the Singlet Fission Process. The RR band of the out-of-plane −CH wagging mode (ν_4 region) becomes symmetrically allowed only upon out-of-plane distortion of the polyene backbone and has been used as a probe for the twist of the carotenoids in the protein scaffold. For a series of carotenoids incorporated in LH complexes from *Rb. sphaeroides* and *Chr. vinosum*,[17] it was demonstrated that the protein dictates the configuration of the carotenoid, irrespective of which one is incorporated. The RR spectra that we measured on the B850 complexes of *Rb. sphaeroides* R-26.1 reconstituted with spheroidene and spirilloxanthin (Figure 2)

follow this notion, as they are markedly similar, showing that the protein environment imposes an identical, planar configuration for both carotenoids, despite the large difference in the extent of their π-electron conjugation. Desamero et al. have also shown that the configuration of spheroidene in the B850:sph complex is very similar to that in the LH2 complex of *Rb. sphaeroides* 2.4.1.[15] The RR spectrum of spirilloxanthin in the LH1 complex of *Rs. rubrum* (Figure 2) shows a much larger and significantly structured ν_4 component, leading to the conclusion that spirilloxanthin in B850:spx is not bound in the same way as by LH1 of *Rs. rubrum* but in a fashion that resembles spheroidene in the LH complexes of *Rb. sphaeroides*.

We observe that the yield of directly generated carotenoid triplets can be related to the conformation of the carotenoid in the LH complexes. In the complexes of *Rb. sphaeroides*, which bind carotenoids in a planar configuration, the triplet is formed with a low yield, of the order of 5−10% in both spirilloxanthin and spheroidene in the B850 complex *Rb. sphaeroides* R-26.1 and in spheroidene in the LH2 complex of *Rb. sphaeroides* 2.4.1.[8] On the other hand, when bound in a twisted configuration in the LH1 complex of *Rs. rubrum*, the triplet yield of spirilloxanthin is significantly higher (25−30%).[7] These observations are consistent with our postulation concerning the mechanism by which triplets arise on an ultrafast timescale. The intramolecular singlet fission mechanism entails the separation of a singlet excited state (S*) into a pair of triplet excitations that coexist on the polyene chain. As was conjectured previously, a distortion or twist of the polyene chain can induce the localization of the two triplets on different parts of the molecule, thus resulting in their separation.[7,8,11] The 3-fold difference in spirilloxanthin triplet yield between the LH1 complex of *Rs. rubrum* and the B850 complex of *Rb. sphaeroides* R-26.1 can be understood as resulting from a distorted configuration of spirilloxanthin in the former and a planar configuration in the latter complex. Thus, the protein matrix controls the light-harvesting function of the carotenoid not only by determining the mutual orientation of carotenoid and BChls but also by regulating the singlet fission reaction pathway from S*. By imposing a planar configuration on the carotenoid, its light-harvesting function is favored by decreasing the probability of the singlet fission process from S*, thus enabling the excited-state energy to flow to BChl. A twisted conformation results in an enhanced fission probability, and the excited-state energy of S* is deactivated by transformation into a triplet pair, which cannot be utilized for photochemical conversion processes and will remain in the antenna until it decays by intersystem crossing.

Conclusions

We have shown that the newly found S* state of spirilloxanthin and spheroidene[7,8] is also present when they are bound to the carotenoidless B850 LH2-type complex of the *Rb. sphaeroides* R-26.1 mutant. The singlet fission mechanism is active, leading to the direct formation of the carotenoid triplet state within the first picoseconds after excitation. The extent of geometrical deformation of the carotenoid imposed by binding to the LH complexes plays a decisive role in determining the formation yield of the carotenoid triplet and partly determines the light-harvesting function of the carotenoid by either deactivating the excited-state energy of S* by transformation into a triplet pair, or allowing this energy to flow to bacteriochlorophyll. The energy transfer from spheroidene to BChl is greatly influenced by the lack of the B800 bacteriochlorophylls, demonstrating that the LH complexes require the use of all their pigments to maximize the efficiency of energy transfer.

Abbreviations

BChl	bacteriochlorophyll
Rs.	*Rhodospirillum*
Rb.	*Rhodobacter*
LH	light-harvesting
IC	internal conversion
EET	excitation energy transfer
SADS	species-associated difference spectra
ESA	excited state absorption
SE	stimulated emission
B50:sph	spheroidene-reconstituted B850 complex
B850:spx	spirilloxanthin-reconstituted B850 complex

Acknowledgment. E.P. and R.v.G. have been financially supported by The Netherlands Organization for Scientific Research through the Council of Earth and Life Sciences (NWO/ALW). J.K. acknowledges financial support from the Foundation for Fundamental Research on Matter (FOM). The work in the laboratory of H.A.F. is supported by grants from the National Science Foundation (MCB-9816759), the National Institute of Health (GM-30353), and the University of Connecticut Research Foundation. A.G. acknowledges financial support from the Federation of European Biochemical Societies (FEBS).

References and Notes

(1) Sundström, V.; Pullerits, T.; van Grondelle, R. *J. Phys. Chem. B* **1999**, *103*, 2327−2346.

(2) Arellano, J. B.; Bangar Raju, B.; Razi-Naqvi, K. N.; Gillbro, T. *Photochem. Photobiol.* **1998**, *68*, 84−87.

(3) MacDermott, G.; Prince, S. M.; Freer, A. A.; Hawthornthwaite-Lawless, A. M.; Papiz, M. Z.; Cogdell, R. J.; Isaacs, N. W. *Nature* **1995**, *374*, 8012−8023.

(4) Frank, H. A.; Cogdell, R. In *Carotenoids in Photosynthesis*; Young, A., Britton, G., Eds.; Chapmann & Hall: London, 1993; pp 252−326.

(5) Koyama, Y.; Kuki, M.; Andersson, P. O.; Gillbro, T. *Photochem. Photobiol*. **1996**, *63*, 243−256.

(6) Ritz, T.; Damjanovic, A.; Schulten, K.; Zhang, J.-P.; Koyama, Y. *Photosynth. Res.* **2000**, *66*, 125−144.

(7) Gradinaru, C. C.; Kennis, J. T. M.; Papagiannakis, E.; van Stokkum, I. H. M.; Cogdell, R. J.; Fleming, G. R.; Niederman, R. A.; van Grondelle, R. *Proc. Natl. Acad. Sci. U.S.A.* **2001**, *98*, 2364−2369.

(8) Papagiannakis, E.; Kennis, J. T. M.; van Stokkum, I. H. M.; Cogdell, R. J.; van Grondelle, R. *Proc. Natl. Acad. Sci. U.S.A.* **2002**, *99*, 6017−6022.

(9) Frank, H. A.; Desamero, R. Z. B.; Chynwat, V.; Gebhard, R.; van der Hoef, I.; Jansen, F. J.; Lugtenburg, J.; Gosztola, D.; Wasielewski, M. R. *J. Phys. Chem. A* **1997**, *101*, 149−157.

(10) Rademaker, H.; Hoff, A. J.; van Grondelle, R.; Duysens, L. N. M. *Biochim. Biophys. Acta* **1980**, *592*, 240−257.

(11) Tavan, P.; Schulten, K. *Phys. Rev. B* **1987**, *36*, 4337.

(12) Zhang, J.-P.; Fujii, R.; Qian, P.; Inaba, T.; Mizoguchi, T.; Koyama, Y.; Onaka, K.; Watanabe, Y.; Nagae, H. *J. Phys. Chem. B* **2000**, *104*, 3683−3691.

(13) Walla, J. P.; Linden, P. A.; Hsu, C.-P.; Scholes, G.; Fleming, G. R. *Proc. Natl. Acad. Sci. U.S.A.* **2000**, *97*, 10808−10813.

(14) Macpherson, A. N.; Arellano, J. B.; Fraser, N. J.; Cogdell, R. J.; Gillbro, T. *Biophys. J.* **2001**, *80*, 923−930.

(15) Desamero, R. Z. B.; Chynwat, V.; van der Hoef, I.; Jansen, F. J.; Lugtenburg, J.; Gosztola, D.; Wasielewski, M. R.; Cua, A.; Bocian, D. F.; Frank, H. A. *J. Phys. Chem. B* **1998**, *102*, 8151−8162.

(16) Kingma, H. Doctoral thesis, Leiden University, Leiden, The Netherlands, 1983.

(17) Noguchi, T.; Hayashi, H.; Tasumi, M. *Biochim. Biophys. Acta* **1990**, *1017*, 280−290.

(18) Gradinaru, C. C.; van Stokkum, I. H. M.; Pascal, A. A.; van Grondelle, R.; van Amerongen, H. *J. Phys. Chem. B* **2000**, *104*, 9330−9342.

(19) van Stokkum, I. H. M.; Scherer, T.; Brouwer, A. M.; Verhoeven, J. W. *J. Phys. Chem.* **1994**, *98*, 852−866.

(20) Frank, H. A. In *The Photochemistry of Carotenoids*; Frank, H. A., Young, A., Britton, G., Cogdell, R., Eds.; Kluwer Academic Publishers: Amsterdam, 1999; pp 235−244.
(21) Lutz, M.; Szponarski, W.; Berger, G.; Robert, B.; Neumann, J. M. *Biochim. Biophys. Acta* **1987**, *894*, 423−424.
(22) Ruban, A. V.; Pascal, A. A.; Robert, B.; Horton, P. *J. Biol. Chem.* **2001**, *276* (27), 24862−70.
(23) Iwata, K.; Hayashi, H.; Tasumi, M. *Biochim. Biophys. Acta* **1985**, *810*, 269−273.
(24) Papagiannakis, E. et al., Manuscript in preparation.